



HAL
open science

Uranium quantification of oak tree rings (*Quercus petraea*) from a former uranium mining site by High Resolution Inductively Coupled Plasma Mass spectrometry in Laser Ablation and Solution modes

Y. Hassan Loni, Karine David, S. Larrue, Bernd Grambow, Christophe Corona, Solange Ribet, P. Chardon, Gilles Montavon

► To cite this version:

Y. Hassan Loni, Karine David, S. Larrue, Bernd Grambow, Christophe Corona, et al.. Uranium quantification of oak tree rings (*Quercus petraea*) from a former uranium mining site by High Resolution Inductively Coupled Plasma Mass spectrometry in Laser Ablation and Solution modes. *Spectrochimica Acta Part B: Atomic Spectroscopy*, 2019, 161, pp.105709. <10.1016/j.sab.2019.105709>. <hal-02406118>

HAL Id: hal-02406118

<https://hal.science/hal-02406118v1>

Submitted on 20 Jul 2022

HAL is a multi-disciplinary open access archive for the deposit and dissemination of scientific research documents, whether they are published or not. The documents may come from teaching and research institutions in France or abroad, or from public or private research centers.

L'archive ouverte pluridisciplinaire **HAL**, est destinée au dépôt et à la diffusion de documents scientifiques de niveau recherche, publiés ou non, émanant des établissements d'enseignement et de recherche français ou étrangers, des laboratoires publics ou privés.



Distributed under a Creative Commons CC BY-NC 4.0 - Attribution - Non-commercial use - International License

1 Uranium quantification of oak tree rings (*Quercus petraea*) from a former uranium mining site by
2 High Resolution Inductively Coupled Plasma Mass spectrometry in Laser Ablation and Solution modes
3 Y. HASSAN LONI¹, K. DAVID^{1*}, S. LARRUE², B. GRAMBOW¹, C. CORONA², S. RIBET¹, P. CHARDON³, and
4 G. MONTAVON¹

5 ¹ Laboratoire SUBATECH, UMR 6457, IN2P3/CNRS/IMT Atlantique/Université de Nantes, 4, rue Alfred
6 Kastler, BP 20722, 44307 Nantes cedex 3, France

7 ² GEOLAB, UMR 6042, CNRS/Université Clermont Auvergne, 4 rue Ledru, 63057 Clermont-Ferrand
8 cedex, France.

9 ³ LPC, UMR 6533, IN2P3/CNRS/Université Clermont Auvergne, 4 avenue Blaise Pascal TSA 60026, CS
10 60026, 63178 Aubière cedex, France.

11 *Corresponding author: karine.david@subatech.in2p3.fr

12 Phone: +33 2 51 85 84 65

13 **Abstract**

14 Tree ring proxies are employed in dendroanalysis as a valuable tool for evaluating past
15 anthropogenic contamination. A wide variety of analytical methods are used to quantify tree ring
16 content for a broad spectrum of chemical elements. Laser Ablation Inductively Coupled Plasma Mass
17 Spectrometry (LA-ICP-MS) is often used to investigate element concentrations in the tree rings.
18 However, several issues regarding the representativeness of laser ablation measurements for trace
19 elements have to be addressed before definitive conclusions can be drawn. In this study, High
20 Resolution (HR)-ICP-MS has been implemented to analyze the trace concentration of uranium (U) in
21 annual growth rings of oak trees (*Quercus Petraea*) using both laser ablation (LA) and solution
22 modes. The three tree samples taken for the present study were located upstream (with respect to
23 the hydrologic system) of a former uranium mine site at Rophin (Puy de Dôme, France), where
24 mining operations were performed between 1949 and 1958. According to the LA-HR-ICP-MS
25 technique, two-dimensional quantitative (2D) mapping of uranium has developed to study the spatial
26 distribution of uranium at the tree ring surface. A strong heterogeneity was observed, leading to an
27 average uranium concentration with high uncertainty (50-66%). Pressed pellets of the standard
28 reference material, NIST1570a spinach leaves and uranium doped cellulose powder were adopted as
29 the uranium standards for quantification. No agreement was found between uranium concentrations
30 measured after acid digestion and the values obtained by laser ablation. This comparison highlights
31 the limitations of laser ablation technique; hence the solution mode should be preferred for
32 quantifying uranium trace concentrations in tree rings. However, low uncertainty (< 9%) was found
33 with the HR-ICP-MS solution, this result should be compared with the deviation observed both at the
34 tree scale ($\approx 40\%$) and across the ≈ 10 m sampling area ($\approx 50\%$).

35 Keywords: HR-ICP-MS, laser ablation, tree rings, uranium mapping, mining activities.

36 **1. Introduction**

37 Dendrochemistry, i.e. the chronological quantification of chemical elements in tree rings, is based on
38 the assumption that element concentrations in the tree-ring series reflect to some degree the
39 chemical signal from the environment during the year of ring formation [1]. As a consequence, these
40 annually resolved and precisely dated proxy records, available over large areas of the earth's land
41 surface, have been widely used to track past and present pollution history. Applications include the
42 biomonitoring of environmental pollution [2], detection and dating of volcanic eruptions [3,4], and

43 reconstruction of longer-term changes in environmental conditions [5–9]. A successful application of
44 dendrochemistry implies that trees chronologically record changes provided the availability of certain
45 elements in their environment. Yet the pathways of uptake and the incorporation and potential
46 relocation of elements in the xylem remain poorly understood and vary widely among tree species
47 [10,11]. More specifically, a careful selection of tree species that minimizes the radial translocation of
48 elements, as well as the radial tendencies in element concentrations from pith to bark and
49 physiological differences between heartwood and sapwood is a prerequisite for the proper use of
50 radial distribution patterns in biomonitoring [12–14]. Moreover, this guarantees the adequacy of
51 dendrochemistry in conducting historical environmental monitoring [15].

52 Dendrogeochemical studies specifically dedicated to uranium are scarce in the scientific literature.
53 Edmands et al. [16] demonstrated the reliability of oak trees growing in a contaminated bog adjacent
54 to a nuclear industrial facility in order to reconstruct shallow groundwater uranium contamination. In
55 Northern Italy, Monticelli et al. [17] detected comparable uranium profiles in *Larix decidua* Miller
56 (European larch) tree-ring series and in Lake Scais sediment cores sampled in the vicinity of the Val
57 Vedello uranium orebody (Orobic Alps). Märten et al. [18] documented the contamination history of
58 an area in Thuringia (Germany) influenced by 40 years of uranium mining and subsequent
59 remediation actions by means of the dendroanalysis of oak trees (*Quercus* sp.). Based on the similar
60 radial uranium distribution patterns of the three trees studied, they concluded the suitability of this
61 technique for investigating past and recent uranium contamination in mining areas. Conversely, in
62 Ohio (USA), Mitchell et al. [19] failed at quantitating the uranium contamination in cores from *Acer*
63 *saccharum*, *Quercus coccinea* and *Populus deltoides* trees growing on the site of a former uranium
64 metal processing facility.

65 Besides the potential interest of this method in reconstructing uranium pollution, as revealed by a
66 majority of the aforementioned studies, another prerequisite herein is the precise and reliable
67 quantification of element concentrations. A wide variety of analytical methods have been used in
68 dendroanalysis to quantify tree-ring content for a broad spectrum of chemical elements, including:
69 Instrumental Neutron Activation Analysis (INAA) [20], Inductively Coupled Plasma Mass Spectrometry
70 (ICP-MS) [21–23], Thermal Ionization Mass Spectrometry (TIMS) [16,24], X-ray fluorescence
71 spectroscopy [25], Proton Induced X-ray Emission [26], and Laser Ablation Inductively Coupled
72 Plasma Mass Spectrometry (LA-ICP-MS) [17,27–29]. A common way to quantify uranium in tree rings
73 is based on the LA-ICP-MS technique [17,18]. LA-ICP-MS does indeed yield a fast direct elemental
74 analysis offering certain advantages, namely it is: (i) selective and nearly non-destructive, (ii)
75 operational with minimal sample preparation required, and (iii) capable of providing high spatial
76 resolution up to 10-100 μm . However, achieving of reliable quantitative measurements can prove to
77 be difficult [30]. The main disadvantage inherent in this technique is its lack of certified reference
78 materials for calibration [29,31–33]. Furthermore, the distribution of the analyte in the sample may
79 also adversely affect the result. It is well known that tree rings are composed of both earlywood and
80 latewood [34]. Also variable densities of the wood inside tree rings were identified, due to
81 seasonality and climate variation [35]. Some researchers have pointed out that tree rings may be
82 viewed as heterogeneous material at the tree ring scale when conducting LA-ICP-MS analyses (e.g.
83 [36]). However, such studies are scarce, and the crucial question about the representativeness of
84 data obtained by laser remains poorly documented.

85 The aim of the present work therefore is twofold: (i) to characterize uranium heterogeneities by
86 developing quantitative two-dimensional (2D) image mapping; and (ii) to compare uranium
87 concentrations obtained by LA-ICP-MS with those derived from solution. The precision of the
88 measurements is discussed in light of the deviation observed both at the tree scale and across the \approx

89 10 m sampling area. The study will enable to determining the best method for a reliable
90 quantification of uranium concentration in tree rings, thus providing clear information for further
91 study on uranium pollution.

92 **2. Materials and Methods**

93 **2.1 Site description and sampling**

94 *2.1.1 Study site*

95 Rophin is one of 17 storage site for of uranium mining residues produced in France during the 20th
96 century. Uranium is a metallic element that naturally occurs in Rophin area.

97 The initial mining activity intended for radium extraction dates back to 1924. Uranium was then
98 extracted from 1948 to 1957 by the French Atomic Energy Commission (CEA). Several other ore
99 bodies, discovered in the vicinity of the Rophin mine, were operated as well, *e.g.* Gagnol (1949-
100 1953), Etang du Reliez (1951-1954), Reliez (1949-1952) and Bancherelle (1952-1954) (see Fig. 1).

101 Between 1948 and 1957, the mechanical leaching of some 44,625 tons of ore produced 33.9 tons of
102 uranium. About 30,000 tons of mine waste are now stored at the site of former Rophin mine (Fig. 2)
103 and covered by vegetation.

104 *2.1.2 Sampling procedure*

105 Oak samples (*Quercus petraea*) were collected from three trees (called T1, T6 and T7) located
106 upstream of the storage residues (*i.e.* not affected by runoff water from mining activities). The trees
107 are separated by a distance of about tens of meters at the same station and lie at an average altitude
108 of 525 m (Fig. 2) and Table S1. (Appendix). However, trees were sampled upstream and downstream
109 from the Rophin site in order to assess past transfer/transport that occurred during mining activities.
110 As part of this methodological development work, we have chosen to work on trees that are not
111 impacted. Only the analytical results of these trees are therefore presented.

112 Tree rings samples were collected on each tree using an increment borer (Pressler inner diameter: 5
113 mm). The selected trees were healthy, grew under similar surrounding natural conditions and belong
114 to the same cohort (*i.e.* germination and growth at roughly the same time, circa 1900). The tree ring
115 samples (n = 5) were extracted from the trunk at about 1.5 m above ground in July 2015. For T6,
116 sampling was performed at three locations about 120° from one another.

117 The sampling strategy allows assessing uranium heterogeneity at the ring level ($\approx \mu\text{m}$ scale), the tree
118 ($\approx \text{m}$ scale) and the local spot where the trees were sampled ($\approx 10 \text{ m}$ scale). Since they are expected
119 not to have been influenced by mining activities, the uranium concentrations should thus be
120 constant and correspond to the geochemical background. Sampling was conducted with great care to
121 avoid any contamination, *i.e.* the borer was washed with ethanol and Milli-Q water between each
122 core extraction. After sampling, all the samples were immediately sealed in individual plastic tubes
123 and transported to the laboratory for dendroanalysis.

124 The tree ring samples were dried at room temperature, and regular abrasive paper (grit 500) was
125 used to polish them. To avoid any cross-ring contamination, the samples were then cleaned of dust
126 by blowing with compressed air.

127 The samples were scanned (1,600 dpi) and the CooRecorder software [37] was run to identify the
128 dating of each ring (to within 1 year). The time period covered by these tree growth rings is: 130
129 years for T1, 118 years for T6, and 152 years for T7. The rings formed in 1958 which correspond to

130 the last year of the on-site uranium mining activity, were arbitrary chosen for purposes of the
131 present work; they were then cut into pieces approx. 2.4 cm in length so as to fit into the laser
132 ablation cell.

133 2.2 Chemicals and reagents

134 Ultrapure water (18.2 MΩ·cm resistivity at 25° and < 5 µg L⁻¹ TOC) obtained from a Milli-Q Advantage
135 A10[®] system (Merck Millipore, France) was used for labware cleaning and preparation of solution
136 analyses. Concentrated nitric acid (HNO₃, 70%, Fischer Scientific) was purified with the Savillex DST-
137 1000 sub-boiling distillation system. Ultrapure NORMATOM[®] 30-32% hydrogen peroxide (H₂O₂)
138 intended for wood acid digestion was purchased from VWR BDH[®] Chemicals. Cellulose powder (20
139 µm granulometry) and standard reference material NIST 1570a spinach leaves intended for direct
140 analyses of uranium by laser ablation HR-ICP-MS were purchased from Sigma Aldrich and the
141 National Institute of Standards and Technology (NIST, USA), respectively. The NIST 612 reference
142 served to optimize the laser operating parameters. Uranium and thallium "PlasmaCAL" stock
143 solutions at 1000 mg L⁻¹, purchased from SCP Science, were used for both calibration and the internal
144 standard solution preparation prior to uranium analyses conducted by HR-ICP-MS in solution mode.

145 2.3 Instrumentation

146 The uranium in tree rings was directly analyzed by LA-HR-ICP-MS with a New Wave Research UP213
147 Nd-YAG laser ablation system (New Wave Research Inc., Huntingdon, Cambridgeshire, UK) coupled to
148 a single-collector sector field ICP-MS instrument (ELEMENT XR, Thermo Scientific, Bremen,
149 Germany).

150 This laser system is equipped with a standard ablation cell (volume 30 cm³) mounted on a motorized
151 xyz stage with sub-micron resolution for sample movement. The target visual inspection is performed
152 by means of a built-in microscope/CCD camera system. The ablation cell was flushed with helium
153 (carrier gas), which transported the laser-induced aerosol to the inductively coupled plasma mass
154 spectrometer.

155 The LA-HR-ICP-MS system was optimized for sensitivity (e.g. gas flows, torch position) prior to sample
156 analysis. The instrument was first tuned in solution mode, and the liquid sample introduction system
157 was then replaced by the laser ablation device with the plasma still switched on.

158 The optimization step in laser mode was carried out using NIST 612 glass reference material with the
159 following laser parameters: raster scan with raster spacing = 100 µm/scan, speed = 5 µm s⁻¹,
160 repetition rate = 10 Hz, laser beam diameter = 80 µm, and laser energy output 60% (1.12 mJ). The
161 helium carrier and argon sample gas flows were adjusted with respect to maximum sensitivity and
162 stability for ⁴³Ca, ¹³⁹La, ²³²Th and ²³⁸U ion signals, as well as for a low ²³²Th¹⁶O/²³²Th ratio (0.03%) and
163 a ²³²Th/²³⁸U ratio close to one. The method's data acquisition set-up in laser mode, including mass
164 offset and peak centering, was carried out with the ablation of NIST 612 at a lower energy output of
165 40% (0.33mJ). The detector cross-calibration was performed using ³⁶Ar.

166 The uranium concentrations of digested sample solutions were measured by HR-ICP-MS, featuring a
167 liquid sample introduction system equipped with an ESI SC-E2 fast system, a Peltier cooler PC³
168 containing a cyclonic spray chamber, a MP² peristaltic pump, and a GE micromist nebulizer. The
169 optimized (LA)-HR-ICP-MS parameters are summarized in Table 1.

170 2.4 Applicable standard and sample preparation procedures

171 2.4.1 Laser ablation HR-ICP-MS

172 The quantification of element concentrations in LA-ICP-MS requires suitable external standards. For
173 tree rings, quantification still presents a challenge because matrix matched standards for calibrations
174 are not available. Consequently, homemade doped cellulose powder with a uranium standard
175 solution was used [27,38,39]. The choice of cellulose powder as an external standard can be justified
176 by the fact that this powder is the major component of wood and moreover its composition is similar
177 to most types of wood. Standard reference material SRM NIST 1570a spinach leaves (U content =
178 $0.155 \pm 0.023 \text{ mg kg}^{-1}$) was introduced as the quality control and external standard.

179 Pellets of uranium-doped cellulose were prepared as follows: 2 g portions of powder were placed
180 into PFA Savillex vials and doped with 10 mL of solution containing various uranium concentrations.
181 The mixture was then shaken with a magnetic stirrer until obtaining a homogeneous solution. Next, it
182 was dried at 80°C until constant weight using the closed evaporation system EvapoClean® (ANALAB)
183 in order to prevent external contamination. The powders were ground in a mixer mill (Retsch MM
184 400, Germany) with 10 mL zirconium oxide (ZrO₂) grinding jars and two 9 mm ZrO₂ balls. The
185 powders were homogenized for 3 min at a frequency of 25 Hz. The grinding parameters were
186 carefully selected in order to obtain the smallest particle size and shortest preparation time. The
187 dried powders were compacted into 13 mm diameter, 2 mm thick disc-shaped pellets at a pressure
188 of 8 tons for 5 min in a Specac® 15T manual hydraulic press. The purchased standard NIST 1570a was
189 transformed into pellets according to the same procedure.

190 The accuracy of the calibration step was verified by analyzing the pellets output. The uranium
191 content was checked by means of HR-ICP-MS after microwave acid digestion using Anton Paar
192 Multiwave 3000®. Results are displayed in Table 2; they are in close agreement (within measurement
193 uncertainty (2σ)) with the gravimetric concentration values for both external standards.

194 In order to fit the samples into the ablation cell, tree core samples were cut into pieces approx. 2.4
195 cm long as indicated above (a mark was applied to identify the ring location). They were then fixed
196 with Araldite® crystal adhesive onto an epoxy mount. The choice of ¹³C as the internal standard for
197 the external quantification method by LA-ICP-MS is common in dendroanalytical studies
198 [14,27,28,40]. Indeed, carbon is widely used as internal standard when analyzing organic samples by
199 LA-ICP-MS due to its uniformity across samples and its natural variation in wood can be neglected,
200 since it is in the per-mille range [41]. Internal standardization allows correcting for various ablation
201 efficiencies, matrix effects, differences in transport efficiency, and wood density properties [42].
202 Furthermore, the ¹³C signal intensity in tree rings has the same order of magnitude as that those
203 measured in cellulose and SRM NIST 1570a. However, ¹³C must be applied with caution; indeed, Frick
204 and Günther [43] have shown that carbon is not an optimal internal standard, as its transport into
205 the ICP can partly occur in the form of carbon dioxide, which will lead to transport properties and
206 efficiencies that can markedly differ from those elements that are transported as particulate matter
207 only. Despite this criticism, ¹³C has been shown to be a suitable internal standard due to its
208 considerable concentration and relatively homogeneous distribution. In addition, evidence of the
209 previous study on trace element analyses in tree rings questioning the use of carbon as internal
210 standard are not reported. Nonetheless, carbon concentrations in samples and standards should be
211 determined with precision. The analyses were carried out with a Thermo Scientific Flash 2000
212 CHNS/O elemental analyzer, and the results are 39.9 ± 0.9 ; 42.2 ± 0.2 ; $46 \pm 1 \text{ \% w}^{-1} (\pm 2\sigma)$ for NIST
213 1570a, Cellulose pellets and tree rings respectively. The average carbon content (n = 5) found in
214 wood exceeds that for cellulose powder by about 10% and that for NIST 1570a by some 14%. This
215 difference between wood and cellulose powder is greater than expected (by about 5%, value given in
216 Hoffman et al. [27]).

217 2.4.2 HR-ICP-MS in solution mode

218 For the acid digestion of samples, individual rings were cut using a sterilized scalpel washed in
219 ethanol and 5% (v/v) nitric acid and then rinsed with Milli-Q water between cuts. The obtained
220 samples weights are respectively: 30, 31, 27, 24 and 12 mg for T1, T6-a, T6-b, T6-c and T7. The
221 mineralization procedure was adapted from that described by Bukata and Kyser [44] which is suitable
222 for these low mass samples. The wood sections were washed in 0.1 M nitric acid for roughly 1 h and
223 then dried in an oven for 7 h at 70°C. Afterwards, the samples were weighed in a 5 mL Savillex
224 container and 1 mL of concentrated HNO₃ was added. The containers were placed into an oven at 80
225 °C for one day and then 0.5 mL of ultra-pure 30% H₂O₂ was added and placed in the oven for an
226 additional day. Once samples were digested, the solutions were cooled down and then diluted in
227 0.35 M HNO₃ using the working solution of internal standard prepared at a concentration of 50 ng L⁻¹.
228 Suitability and accuracy of the method were tested through digested NIST 1570a with same
229 procedure.

230 The external calibration solutions with uranium concentrations ranging from 10 to 50 ng L⁻¹ were
231 prepared by diluting uranium stock standard solution with 50 ng L⁻¹ Tl solution in 0.35M HNO₃. The
232 correlation coefficient (R²) values of calibration curves were between 0.999 and 1.00 over the study
233 duration.

234 **2.5 2D mapping of uranium by LA-HR-ICP-MS**

235 *2.5.1 Identification of tree ring ablation area*

236 Before analyses conducted by LA-ICP-MS, the tree rings were characterized by a Leica DCF290 HD
237 Digital camera in order to locate the optimal ablation area. This step is important as it provides
238 information on the surface structure of the tree ring before the ablation, size and dimension of the
239 samples. All studied samples are shown in Figure 3.

240 The rings are composed of two parts, *i.e.* earlywood and latewood formed respectively during spring
241 and summer/early autumn (until the beginning of the vegetative rest period). Earlywood is porous
242 and characterized by white cells with large diameters, whereas latewood is composed of small cells
243 and densely-layered, strong thick-walled cells. Not all rings are uniform; some are thinner, some
244 thicker, some light and some dark. Among the samples, tree ring widths actually range from 0.7 to 4
245 mm depending on seasonal conditions, e.g. rainfall, temperature, and soil nutrients.

246 For the sake of optimization and representativeness, latewood was chosen in order to allow a
247 maximum amount of material to be ablated; moreover 1 mm² surface (constant across all rings) was
248 chosen with an ablation pattern containing 56 lines. Note that the digested part for uranium
249 measurements by HR-ICP-MS solution also corresponds to latewood.

250 *2.5.2 Laser data processing and automation of 2D quantitative uranium mapping at tree ring surface*

251 The HR-ICP-MS was synchronized with the laser ablation device in external trigger mode. Then the
252 optimum LA-HR-ICP-MS method developed for quantitative uranium mapping was used (see Table 1
253 for operational details). Prior to actual data acquisition, a pre-ablation was performed to remove any
254 surface contamination. The tree rings were laser ablated through the use of single line patterns. The
255 quantitative 2D uranium images were obtained from 56 lines (7 x 8) of ablation, and the total ablated
256 surface was approx. 1 mm². The analysis allowed measuring of 55 scans in 1 min, with 20 s of sample
257 acquisition during laser ablation once the laser was fired and 40 s of background collection with no
258 ablation. Overall, the total analysis time by sample was about 2 h. Due to the slow aerosol washout
259 time (50 s) already mentioned elsewhere [45], the spatial resolution was limited (100 μm(x)-80
260 μm(y)). The tree ring analyses were bracketed by standard measurements (five lines per standard).

261 ^{238}U and ^{13}C time-resolved raw data were exported from the HR-ICP-MS in ASC or FIN format (Glitter
 262 software users) and processed offline using a series of in-house subroutines written in VBA language
 263 for Microsoft Excel 2010™. The average gas blank signal intensities for all elements recorded without
 264 laser ablation were calculated and then subtracted from the signal intensities measured during
 265 standard and sample ablation. The ^{238}U signal intensity at each time slice was normalized relative to
 266 the internal standard ^{13}C signal intensity, and both the average and standard error of the normalized
 267 ratio were calculated after an iterative procedure to remove outliers by means of the modified
 268 Thompson τ test [46,47]. A time drift correction was applied with a linear interpolation over time in
 269 using normalized ^{238}U signal intensities from the bracketing standard reference materials. The
 270 uranium concentration and associated error ($k=1$) of each analysis were calculated from the
 271 following equations below:

$$272 \quad [\text{U}]_{\text{SMP}} = [\text{U}]_{\text{STD}} \times \frac{[\text{C}]_{\text{SMP}}}{[\text{C}]_{\text{STD}}} \times \frac{\bar{I}_{\text{U}}^{\text{SMP}}}{\bar{I}_{\text{C}}^{\text{SMP}}} \times \frac{(N_2 - N_1)}{\left[\left[\left(\frac{\bar{I}_{\text{U}}^{\text{STD}}}{\bar{I}_{\text{C}}^{\text{STD}}} \right)_1 \times (N_2 - N_i) \right] + \left[\left(\frac{\bar{I}_{\text{U}}^{\text{STD}}}{\bar{I}_{\text{C}}^{\text{STD}}} \right)_2 \times (N_i - N_1) \right] \right]}$$

273 where $[\text{U}]_{\text{SMP,STD}}$ and $[\text{C}]_{\text{SMP,STD}}$ are the uranium and carbon contents in the sample (SMP) and
 274 standard reference material (STD); $\frac{\bar{I}_{\text{U}}^{\text{SMP}}}{\bar{I}_{\text{C}}^{\text{SMP}}}$ the average normalized ^{238}U intensity signal in sample;
 275 $\left(\frac{\bar{I}_{\text{U}}^{\text{STD}}}{\bar{I}_{\text{C}}^{\text{STD}}} \right)_{1,2}$ the average normalized ^{238}U intensity signals measured in bracketing standards 1 and 2; and
 276 N_1 , N_2 and N_i are the analysis numbers in the sequence.

277

278

$$279 \quad \text{Err}[\text{U}]_{\text{SMP}} = [\text{U}]_{\text{SMP}} \times \sqrt{\left(\frac{\text{Err}[\text{U}]_{\text{STD}}}{[\text{U}]_{\text{STD}}} \right)^2 + \left(\frac{\text{Err}[\text{C}]_{\text{SMP}}}{[\text{C}]_{\text{SMP}}} \right)^2 + \left(\frac{\text{Err}[\text{C}]_{\text{STD}}}{[\text{C}]_{\text{STD}}} \right)^2 + \left(\frac{\text{Err} \left(\frac{\bar{I}_{\text{U}}^{\text{SMP}}}{\bar{I}_{\text{C}}^{\text{SMP}}} \right)}{\left(\frac{\bar{I}_{\text{U}}^{\text{SMP}}}{\bar{I}_{\text{C}}^{\text{SMP}}} \right)} \right)^2 + \left(\frac{\text{Err} \left(\frac{\bar{I}_{\text{U}}^{\text{STD}}}{\bar{I}_{\text{C}}^{\text{STD}}} \right)}{\left(\frac{\bar{I}_{\text{U}}^{\text{STD}}}{\bar{I}_{\text{C}}^{\text{STD}}} \right)} \right)^2}$$

$$280 \quad \text{with} \quad \left(\frac{\text{Err} \left(\frac{\bar{I}_{\text{U}}^{\text{STD}}}{\bar{I}_{\text{C}}^{\text{STD}}} \right)}{\left(\frac{\bar{I}_{\text{U}}^{\text{STD}}}{\bar{I}_{\text{C}}^{\text{STD}}} \right)} \right)^2 = \frac{\left(\text{Err} \left(\frac{\bar{I}_{\text{U}}^{\text{STD}}}{\bar{I}_{\text{C}}^{\text{STD}}} \right)_1 \times (N_2 - N_i) \right)^2 + \left(\text{Err} \left(\frac{\bar{I}_{\text{U}}^{\text{STD}}}{\bar{I}_{\text{C}}^{\text{STD}}} \right)_2 \times (N_i - N_1) \right)^2}{\left[\left(\frac{\bar{I}_{\text{U}}^{\text{STD}}}{\bar{I}_{\text{C}}^{\text{STD}}} \right)_1 \times (N_2 - N_i) + \left(\frac{\bar{I}_{\text{U}}^{\text{STD}}}{\bar{I}_{\text{C}}^{\text{STD}}} \right)_2 \times (N_i - N_1) \right]^2}$$

281

282 Where Err are the standard deviations ($k=1$) calculated from measured values (carbon concentrations
 283 in sample and standards, normalized ^{238}U signal intensities, gravimetric values (uranium
 284 concentrations in homemade standards) and reported by NIST (uranium concentration in the
 285 NIST1570a standard).

286 The quantitative two-dimensional mappings of the uranium distribution were obtained by plotting
 287 the signal intensity of each line based on the recalculated coordinate. 2D images were built by
 288 processing data with the Origin 8.6® software.

289 2.6 Limits of detection (LOD)

290 The limits of detection (LODs) of the LA-HR-ICP-MS for uranium were calculated based on 3 standard
291 deviations (sd) of gas blank ^{238}U signal intensity measurements from five replicate analyses of NIST
292 1570a. In solution mode, the LODs were calculated over 3 standard deviations of the intercept
293 parameter of the calibration line.

294 The LODs of uranium for both instrumental techniques were determined and listed in Table 3. The
295 LODs for laser ablation range from 7 to 24 ng kg^{-1} , which is between approx. 20 and 100 times higher
296 than those found in solution mode. This difference is primarily owed to the greater variability in
297 signal intensities for LA compared with solution mode. In addition, the amount (mass) of sample
298 transported into the plasma by LA is less than that in solution mode despite the dilution factor of the
299 latter [48].

300 **3. Results and discussion**

301 **3.1 Uranium distribution in tree rings**

302 Uranium is present in plants despite the fact that it performs no known metabolic function [19]; in
303 living systems, it even has a clearly toxic function. Since uranium does not constitute a main tree
304 nutrient, it is found in low concentrations. To obtain the spatial distribution of uranium in the tree
305 rings, the samples were pasted onto an epoxy support, scanned line by line with a focused laser
306 beam and ultimately analyzed by HR-ICP-MS. The two-dimensional images (signal of $(^{238}\text{U}/^{13}\text{C})$) and
307 histograms of uranium concentration distribution are shown in Figure 4. The spatial resolution of 2D
308 images depends on the integration time of the mass spectrometer instrument as well as on the
309 washout time of the laser-generated aerosol through the transport system, including the ablation cell
310 and transport tubing [49]. Furthermore, the signal obtained by LA-ICP-MS is not directly attributable
311 to a specific location on the sample due to the involvement of sample transport and diffusion, unless
312 considerable care is taken during the analysis [50]. The figures obtained show that the uranium
313 distribution at the ring scale is indeed heterogeneous, leading to a mean concentration with a
314 significant associated error (1σ) on the order of 50% to 66% (prior to the rejection of outliers).
315 Moreover, the uranium distribution differs in each sample; it appears to be nearly homogeneously
316 distributed in tree ring T1, whereas in the other samples, the distribution seems quite
317 heterogeneous. A recent study [51] evaluated the distribution of some elements in the tree rings of
318 *Tipuana tipu* (*Fabaceae*). Results revealed a non-random distribution of these chemical elements
319 within the rings, with a higher content in the cell walls of vessels and lower content in the fibers. In
320 our case, uranium appears to be highly concentrated ($> 200 \mu\text{g kg}^{-1}$) in some parts of tree rings (hot
321 spots), yet no correlation was observed between these "hot spots" and any specific tree ring
322 location. The reasons for these localized maxima are unclear and the mechanism that controls
323 uranium distribution is not yet known well enough to explain these observations. We can however
324 hypothesize that this may be correlated with the tree ring anatomy. Tree rings can indeed be
325 considered as heterogeneous or multi-phase samples (see Fig. 3), and trace elements taken up by a
326 tree are fixed depending on their affinity to the different tree ring cells causing this heterogeneity.
327 This assumption undoubtedly requires more substantiation. However, Narewski *et al.* [52] found that
328 the elements present at higher concentrations (major elements) in bark samples are characterized by
329 relative standard deviations (RSD) of the average concentration below 15%; for elements with much
330 lower average concentrations, higher RSD values between 20% and 30% were obtained. Further
331 studies are needed to gain more complete information. Nonetheless, an inhomogeneous elemental
332 distribution leads to poor measurement precision and can result in a non-representative sampling by
333 laser [53]. Data accuracy and interpretation (i.e. the quantitative analysis) can also be called into
334 question. This aspect will be addressed in greater detail in the following section.

335 3.2 Quantification of analytical data in laser ablation mode

336 Elemental quantification in tree rings by means of LA-HR-ICP-MS is a challenging task because of the
337 difficulty involved in finding a matrix that exactly matches the sample characteristics. In our study,
338 calibration was carried out with two types of pressed pellets, and all count rates were normalized to
339 ^{13}C . A slight difference in uranium content between the two methods of quantification (uranium-
340 doped cellulose pellets and NIST 1570a) was observed (Figure 5). Cellulose pellet heterogeneity at
341 the micron scale was indeed detected, which may explain this difference. The effects of sample
342 grinding time and particle size are closely correlated with sample heterogeneity [31]. The longer the
343 grinding time and the smaller the particle size, the higher the level of measurement precision.
344 Nevertheless, when taking into account the uranium distribution and resulting high measurement
345 uncertainty, this difference is not statistically significant. For the sake of precision, NIST 1570a was
346 used as the external standard for elemental quantification in tree rings by LA-HR-ICP-MS.

347 3.3 Comparison of laser ablation and solution uranium data

348 A comparison between laser ablation and solution data of the tree ring analysis is presented in Figure
349 5. The uranium concentrations measured after acid digestion are significantly different from the
350 average values (from 56 ablation lines) obtained by LA-HR-ICP-MS. This discrepancy can be explained
351 by sample inhomogeneity, which was highlighted by the 2D mapping (see Fig. 4). For sample T1,
352 whose uranium is nearly homogeneously distributed, a consistency indeed exists between the result
353 obtained by acid digestion and that recorded by laser ablation, whereas for the other samples, no
354 agreement was found. The uranium concentration is systematically overestimated for LA-HR-ICP-MS,
355 with the relative standard deviation ranging from 50% to 66% (1σ). This finding would indicate that
356 the method adapted to 2D mapping is not adequate for absolute uranium quantification. Although
357 the laser beam has ablated a wide area, the amount of ablated material may not be sufficient for
358 good sample representativeness. The resulting ablated mass strongly depends on both the laser
359 ablation process (scan modes, beam diameter, energy, number of lines or spots, etc.) and sample
360 properties (density, thermal conductivity, etc.). Even though a large number of publications about
361 trace element quantification in tree rings by LA-ICP-MS exists, the ablated mass and sample
362 heterogeneity are seldom discussed. This point may have major consequences for the interpretation
363 of results. Gough and Ridley [54] found, for certain trace elements, that duplicate analyses within a
364 given tree ring indicated a tremendous difference in results. In this case, the possible differences
365 between years (rings) cannot be assessed. In the present work, the ablated mass of material per tree
366 ring equals approx. 1 mg, with this value being of the same order of magnitude as that mentioned by
367 Prohaska *et al.* [55] (1-2 mg), but lower than that of Hoffman *et al.* [27] (≈ 5 mg). Due to the small
368 ablated mass of material, the quantification by LA-ICP-MS for inhomogeneous samples might be
369 limited without any matrix-matched calibration standards. Increasing the level of analytical precision
370 and accuracy while overcoming heterogeneities would require either ablating a significant area in
371 order to produce a sufficiently representative quantity of material or else grinding the wood to fine
372 particles for pressing into laser ablation pellets. The latter approach is not only time-consuming but
373 also a potential source of errors by contamination during sample preparation. Since quantification by
374 laser ablation for heterogeneously-distributed tree ring elements appears to be a complicated issue,
375 the literature contains only a very limited discussion on comparisons of elemental quantification in
376 tree rings by ICP-MS laser ablation and ICP-MS solution. Nonetheless, Hoffman *et al.* [27] and
377 Watmough *et al.* [36] did find good agreement between acid digestions values and values obtained
378 by laser ablation for tree ring samples. Despite these findings, the Hoffman *et al.* work mentioned
379 that the ablation process is complex and undermines both accuracy and calibration, while Watmough
380 *et al.* indicated that elemental concentrations recorded by laser ablation are likely to differ slightly

381 from those recorded by acid digestion. Laser ablation can certainly become more representative
382 when vaporizing a sufficiently large sample mass, but the most accurate method at the tree ring level
383 is its digestion. The solution mode was thus chosen for the following section. If measurement
384 accuracy at the ring level is important, then this aspect must be "balanced" against the elemental
385 distribution heterogeneity in the ring at the level of the entire tree and the sampling area. This
386 aspect will be discussed below.

387 **3.4 Uranium concentration in rings at the level of the entire tree and sampling area**

388 In growth ring T6, uranium was measured at three locations along the circular path of the tree ring
389 (figure 5). For the same ring sampled at different trunk locations (at the same height), the uranium
390 concentration only varies slightly. Here, the mean uranium concentration for all three T6 samples
391 equals: 5.2 ± 2.2 (1σ) $\mu\text{g kg}^{-1}$. However, this variation is smaller than that obtained by Prohaska *et al.*
392 [38] (up to 60%), which was explained by the changing proportion of compression wood on the
393 various sides of the tree stem. In this study, the analyzed tree T6 is not affected by compression,
394 mainly due to the wind, slope or proximity to another tree. The deviation ($\approx 40\%$) is much higher
395 than the post-digestion measurement precision ($< 9\%$); a comparison should be drawn with the
396 deviation at the sample location spot. The uranium concentrations recorded in the three trees are of
397 the same order of magnitude, with a mean concentration of: 4.5 ± 2.2 (1σ) $\mu\text{g kg}^{-1}$. The deviation
398 (roughly 50%) however is also much higher than that obtained for a single tree ring. Although it is
399 important for trace element measurement uncertainty in the tree rings to be low, this condition
400 must be placed in perspective if deviation at the sample location site is significant.

401 **4. Conclusion**

402 LA-HR-ICP-MS and HR-ICP-MS solution mode have been applied to measure uranium concentration
403 in oak tree rings. No agreement between the results obtained with these two techniques was found,
404 except for one sample (T1_1958). While LA-ICP-MS is often used in the literature to quantify
405 elements in tree rings, these investigations have shown that before implementing laser ablation, it
406 should first be clarified whether the sample is sufficiently homogeneous to produce representative
407 results. Laser ablation only becomes worthwhile if certain conditions are met. In the present work,
408 the uranium distribution in tree rings was found to be very heterogeneous, a finding highlighted by
409 the 2D mapping that led to average values being associated with significant uncertainty (50% to
410 66%). Note that quantification is feasible with commercially available spinach leaves meeting the
411 NIST 1570a Standard. The origin of this heterogeneous uranium distribution has yet to be well
412 understood, but it may be related to the low concentration values. As regards quantification by laser
413 ablation, the mean value is overestimated, in association with significant error. The ICP-MS solution
414 is therefore preferable for the absolute quantification of trace elements in tree rings; even though
415 sample preparation is labor intensive and can increase the likelihood of contamination, it is much
416 more sensible and offers lower uncertainty ($< 9\%$). This consideration however should be treated
417 with caution. At the tree level, uranium concentration may vary as a function of location along the
418 circular path of the tree ring, leading to a mean concentration with an RSD of approx. 40%.
419 Compared to the deviation ($\approx 50\%$) at the sample location level, it is preferable to use the same tree
420 ring to analyze several samples taken from different trunk locations and then average the results.
421 The ICP-MS solution measurement will provide an accurate quantitative value at the level of the ring
422 whereas the measurement average will give a good concentration representativeness at the level of
423 the tree.

424 In contrast, laser ablation is a powerful technique for developing quantitative 2D mapping; this
425 technique may improve understanding of the trace element distribution mechanisms in tree rings.

426 Laser ablation remains preferable when the tree ring is narrow and impossible to be cut, in which
427 case heterogeneity must be taken into account. It is recommended to make several ablation lines (or
428 spots) in order to cover a large tree ring area.

429 **Acknowledgments**

430 This work has received financial support from France's *Pays de la Loire* Regional Council (as part of
431 the RS2E-OSUNA project). This work was part of a research program performed in the frame of the
432 "Zone Atelier Territoires Uranifères"

433 The authors would like to thank C. Fonquernie from *Laboratoire Magmas et Volcans* (Clermont-
434 Ferrand, France) for the carbon analyses and the two anonymous reviewers for their helpful and
435 constructive comments that greatly improved the final version of the manuscript.

436 **References**

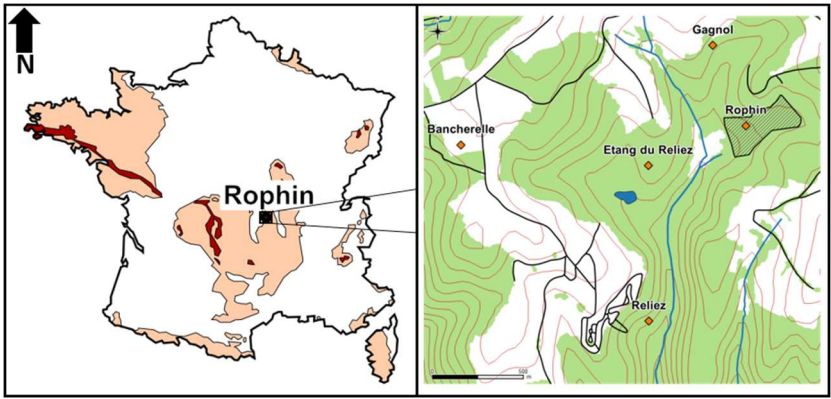
- 437 [1] J. Hagemeyer, Chapter 13 Trace metals in tree rings: what do they tell us?, *Trace Met.*
438 *Environ.* 4 (2000) 375–385. doi:10.1016/S0927-5215(00)80016-8.
- 439 [2] J.G. Burken, D.A. Vroblesky, J.C. Balouet, *Phytoforensics, Dendrochemistry, and*
440 *Phytoscreening: New Green Tools for Delineating Contaminants from Past and Present,*
441 *Environ. Sci. Technol.* 45 (2011) 6218–6226. doi:10.1021/es2005286.
- 442 [3] C. Pearson, S.W. Manning, M. Coleman, K. Jarvis, Can tree-ring chemistry reveal absolute
443 dates for past volcanic eruptions?, *J. Archaeol. Sci.* 32 (2005) 1265–1274.
444 doi:10.1016/J.JAS.2005.03.007.
- 445 [4] C.L. Pearson, D.S. Dale, P.W. Brewer, P.I. Kuniholm, J. Lipton, S.W. Manning, Dendrochemical
446 analysis of a tree-ring growth anomaly associated with the Late Bronze Age eruption of Thera,
447 *J. Archaeol. Sci.* 36 (2009) 1206–1214. doi:10.1016/J.JAS.2009.01.009.
- 448 [5] T.W. Berger, G. Köllensperger, R. Wimmer, Plant-soil feedback in spruce (*Picea abies*) and
449 mixed spruce-beech (*Fagus sylvatica*) stands as indicated by dendrochemistry, *Plant Soil.* 264
450 (2004) 69–83. doi:10.1023/B:PLSO.0000047714.43253.25.
- 451 [6] Y. Kuang, G. Zhou, D. Wen, Environmental bioindication of sulfur in tree rings of Masson pine
452 (*Pinus massoniana* L.) in the Pearl River Delta of China, *Front. For. China.* 4 (2009) 1–6.
453 doi:10.1007/s11461-009-0003-9.
- 454 [7] S.A. Watmough, T.C. Hutchinson, Analysis of tree rings using inductively coupled plasma mass
455 spectrometry to record fluctuations in a metal pollution episode, *Environ. Pollut.* 93 (1996)
456 93–102. doi:10.1016/0269-7491(95)00107-7.
- 457 [8] J.G.A. Lageard, J.A. Howell, J.J. Rothwell, I.B. Drew, The utility of *Pinus sylvestris* L. in
458 dendrochemical investigations: Pollution impact of lead mining and smelting in Darley Dale,
459 Derbyshire, UK, *Environ. Pollut.* 153 (2008) 284–294. doi:10.1016/J.ENVPOL.2007.08.031.
- 460 [9] Y. Liu, W. Ta, P. Cherubini, R. Liu, Y. Wang, C. Sun, Elements content in tree rings from Xi'an,
461 China and environmental variations in the past 30 years, *Sci. Total Environ.* 619–620 (2018)
462 120–126. doi:10.1016/J.SCITOTENV.2017.11.075.
- 463 [10] B.E. Cutter, R.P. Guyette, Anatomical, Chemical, and Ecological Factors Affecting Tree Species
464 Choice in Dendrochemistry Studies, *J. Environ. Qual.* 22 (1993) 611–619.
465 doi:10.2134/jeq1993.00472425002200030028x.
- 466 [11] K. T Smith, W. C Shortle, U.F. Service, N. Forest, E. Station, P. O Box, Tree biology and
467 dendrochemistry, *Environment.* (1996) 629–635.

- 468 [12] S.A. Watmough, T.C. Hutchinson, R.D. Evans, Application of Laser Ablation Inductively Coupled
469 Plasma–Mass Spectrometry in Dendrochemical Analysis, *Environ. Sci. Technol.* 31 (1997) 114–
470 118. doi:10.1021/es960168d.
- 471 [13] C. Nabais, H. Freitas, J. Hagemeyer, S.-W. Breckle, Radial distribution of Ni in stemwood of
472 *Quercus ilex* L. trees grown on serpentine and sandy loam (umbric leptosol) soils of NE-
473 Portugal, *Plant Soil.* 183 (1996) 181–185. doi:10.1007/BF00011433.
- 474 [14] C.-D. Garbe-Schönberg, C. Reimann, V.A. Pavlov, Laser ablation ICP-MS analyses of tree-ring
475 profiles in pine and birch from N Norway and NW Russia -- a reliable record of the pollution
476 history of the area?, *Environ. Geol.* 32 (1997) 9–16. doi:10.1007/s002540050188.
- 477 [15] S.N. Abreu, A.M.V.M. Soares, A.J.A. Nogueira, F. Morgado, Tree Rings, *Populus nigra* L., as
478 Mercury Data Logger in Aquatic Environments: Case Study of an Historically Contaminated
479 Environment, *Bull. Environ. Contam. Toxicol.* 80 (2008) 294–299. doi:10.1007/s00128-008-
480 9366-0.
- 481 [16] J.D. Edmands, D.J. Brabander, D.S. Coleman, Uptake and mobility of uranium in black oaks:
482 Implications for biomonitoring depleted uranium-contaminated groundwater, *Chemosphere.*
483 44 (2001) 789–795. doi:10.1016/S0045-6535(00)00376-3.
- 484 [17] D. Monticelli, A. Di Iorio, E. Ciceri, A. Castelletti, C. Dossi, Tree ring microanalysis by LA--ICP--
485 MS for environmental monitoring: validation or refutation? Two case histories, *Microchim.*
486 *Acta.* 164 (2009) 139–148. doi:10.1007/s00604-008-0049-7.
- 487 [18] A. Märten, D. Berger, M. Köhler, D. Merten, The dendroanalysis of oak trees as a method of
488 biomonitoring past and recent contamination in an area influenced by uranium mining,
489 *Environ. Sci. Pollut. Res.* 22 (2015) 19417–19425. doi:10.1007/s11356-015-4902-z.
- 490 [19] T. Mitchell, P. Sandwall, B. Rolfes, M. Lobaugh, J. Bowen, J. Elliston, S. Glover, H. Spitz,
491 Feasibility of using dendroanalysis of uranium as a biomarker for environmental
492 contamination, *J. Radioanal. Nucl. Chem.* 277 (2008) 223–225. doi:10.1007/s10967-008-0734-
493 3.
- 494 [20] J.C. Sheppard, W.H. Funk, Trees as Environmental Sensors Monitoring Long-Term Heavy Metal
495 Contamination of Spokane River, Idaho, *Environ. Sci. Technol.* 9 (1975) 638–642.
496 doi:10.1021/es60105a006.
- 497 [21] K.-F. Yu, B.S. Kamber, M.G. Lawrence, A. Greig, J.-X. Zhao, High-precision analysis on annual
498 variations of heavy metals, lead isotopes and rare earth elements in mangrove tree rings by
499 inductively coupled plasma mass spectrometry, *Nucl. Instruments Methods Phys. Res. Sect. B*
500 *Beam Interact. with Mater. Atoms.* 255 (2007) 399–408. doi:10.1016/J.NIMB.2006.11.127.
- 501 [22] L.E. Beramendi-Orosco, M.L. Rodriguez-Estrada, O. Morton-Bermea, F.M. Romero, G.
502 Gonzalez-Hernandez, E. Hernandez-Alvarez, Correlations between metals in tree-rings of
503 *Prosopis juliflora* as indicators of sources of heavy metal contamination, *Appl. Geochemistry.*
504 39 (2013) 78–84. doi:10.1016/j.apgeochem.2013.10.003.
- 505 [23] O. Morton-Bermea, L. Beramendi-Orosco, Á. Martínez-Reyes, E. Hernández-Álvarez, G.
506 González-Hernández, Increase in platinum group elements in Mexico City as revealed from
507 growth rings of *Taxodium mucronatum* ten, *Environ. Geochem. Health.* 38 (2016) 195–202.
508 doi:10.1007/s10653-015-9703-2.
- 509 [24] K.C. McHugh, E. Widom, H.B. Spitz, S.E. Glover, Analysis of a sugar maple tree core for
510 monitoring environmental uranium contamination, *J. Radioanal. Nucl. Chem.* 307 (2016)
511 1691–1696. doi:10.1007/s10967-015-4369-x.

- 512 [25] T. Scharnweber, A. Hevia, A. Buras, E. van der Maaten, M. Wilmking, Common trends in
513 elements? Within- and between-tree variations of wood-chemistry measured by X-ray
514 fluorescence — A dendrochemical study, *Sci. Total Environ.* 566–567 (2016) 1245–1253.
515 doi:10.1016/J.SCITOTENV.2016.05.182.
- 516 [26] J.R. McClenahan, J.P. Vimmerstedt, A.J. Scherzer, Elemental concentrations in tree rings by
517 PIXE: statistical variability, mobility, and effects of altered soil chemistry, *Can. J. For. Res.* 19
518 (1989) 880–888. doi:10.1139/x89-134.
- 519 [27] E. Hoffmann, C. Lüdke, H. Scholze, H. Stephanowitz, Analytical investigations of tree rings by
520 laser ablation ICP-MS, *Fresenius. J. Anal. Chem.* 350 (1994) 253–259.
521 doi:10.1007/BF00322478.
- 522 [28] S.A. Watmough, T.C. Hutchinson, R.D. Evans, Development of Solid Calibration Standards for
523 Trace Elemental Analyses of Tree Rings by Laser Ablation Inductively Coupled Plasma-Mass
524 Spectrometry, *Environ. Sci. Technol.* 32 (1998) 2185–2190. doi:10.1021/es980008x.
- 525 [29] A. Perone, C. Cocozza, P. Cherubini, O. Bachmann, M. Guillong, B. Lasserre, M. Marchetti, R.
526 Tognetti, Oak tree-rings record spatial-temporal pollution trends from different sources in
527 Terni (Central Italy), *Environ. Pollut.* 233 (2018) 278–289. doi:10.1016/J.ENVPOL.2017.10.062.
- 528 [30] M.A.O. Da Silva, M.A.Z. Arruda, Laser ablation (imaging) for mapping and determining Se and
529 S in sunflower leaves, *Metallomics.* 5 (2013) 62–67. doi:10.1039/c2mt20154b.
- 530 [31] M.S. Jiménez, M.T. Gómez, J.R. Castillo, Multi-element analysis of compost by laser ablation-
531 inductively coupled plasma mass spectrometry, *Talanta.* (2007).
532 doi:10.1016/j.talanta.2007.01.006.
- 533 [32] H.-J. Stärk, R. Wennrich, A new approach for calibration of laser ablation inductively coupled
534 plasma mass spectrometry using thin layers of spiked agarose gels as references, *Anal.*
535 *Bioanal. Chem.* 399 (2011) 2211–2217. doi:10.1007/s00216-010-4413-1.
- 536 [33] M.A.G. Nunes, M. Voss, G. Corazza, E.M.M. Flores, V.L. Dressler, External calibration strategy
537 for trace element quantification in botanical samples by LA-ICP-MS using filter paper, *Anal.*
538 *Chim. Acta.* 905 (2016) 51–57. doi:10.1016/j.aca.2015.11.049.
- 539 [34] T. Higuchi, *Biochemistry and Molecular Biology of Wood*, Springer, 1997. doi:10.1007/978-3-
540 642-60469-0.
- 541 [35] A. Moberg, D.M. Sonechkin, K. Holmgren, M.H. Datsenko, W. Karlén, Highly variable Northern
542 Hemisphere temperatures reconstructed from low- and high-resolution proxy data, *Nature.*
543 433 (2005) 613–617. doi:10.1038/nature03265.
- 544 [36] S.A. Watmough, T.C. Hutchinson, R.D. Evans, Application of laser ablation inductively coupled
545 plasma-mass spectrometry in dendrochemical analysis, *Environ. Sci. Technol.* 31 (1997) 114–
546 118. doi:10.1021/es960168d.
- 547 [37] Lars-Åke Larsson, CDendro & CooRecorder Program Package for Tree Ring Measurements and
548 Crossdating of the Data, (2016). <http://www.cybis.se/forfun/dendro/>.
- 549 [38] T. Prohaska, C. Stadlbauer, R. Wimmer, G. Stingeder, C. Latkoczy, E. Hoffmann, H.
550 Stephanowitz, Investigation of element variability in tree rings of young Norway spruce by
551 laser-ablation-ICPMS, *Sci. Total Environ.* 219 (1998) 29–39. doi:10.1016/S0048-
552 9697(98)00224-1.
- 553 [39] T. Barrelet, A. Ulrich, H. Rennenberg, C.N. Zwicky, U. Krähenbühl, Assessing the suitability of
554 Norway spruce wood as an environmental archive for sulphur, *Environ. Pollut.* 156 (2008)

- 555 1007–1014. doi:10.1016/J.ENVPOL.2008.05.004.
- 556 [40] K. Kyser, D. Chipley, A. Bukata, P. Polito, A. Fitzpatrick, P. Alexandre, Application of Laser
557 Ablation and High Resolution ICPMS to the Analysis of Metal Contents in Tree Rings, Ages of
558 Uranium-rich minerals and Se Contents in Sulphide Ores, *Can. J. Anal. Sci. Spectrosc.* 48 (2003)
559 258–268.
- 560 [41] A. Duquesnay, N. Bréda, M. Stievenard, J.L. Dupouey, Changes of tree-ring $\delta^{13}\text{C}$ and water-
561 use efficiency of beech (*Fagus sylvatica* L.) in north-eastern France during the past century,
562 *Plant, Cell Environ.* 21 (1998) 565–572. doi:10.1046/j.1365-3040.1998.00304.x.
- 563 [42] T. Barrelet, A. Ulrich, H. Rennenberg, U. Krähenbühl, Seasonal Profiles of Sulphur, Phosphorus,
564 and Potassium in Norway Spruce Wood, *Plant Biol.* 8 (2006) 462–469. doi:10.1055/s-2006-
565 924044.
- 566 [43] D.A. Frick, D. Günther, Fundamental studies on the ablation behaviour of carbon in LA-ICP-MS
567 with respect to the suitability as internal standard, *J. Anal. At. Spectrom.* 27 (2012) 1294.
568 doi:10.1039/c2ja30072a.
- 569 [44] A.R. Bukata, T.K. Kyser, Tree-ring elemental concentrations in oak do not necessarily passively
570 record changes in bioavailability, *Sci. Total Environ.* 390 (2008) 275–286.
571 doi:10.1016/J.SCITOTENV.2007.09.005.
- 572 [45] D. Frei, A. Gerdes, Precise and accurate in situ U-Pb dating of zircon with high sample
573 throughput by automated LA-SF-ICP-MS, *Chem. Geol.* (2009).
574 doi:10.1016/j.chemgeo.2008.07.025.
- 575 [46] W.R. Thompson, On a criterion for the rejection of observations and the distribution of the
576 ratio of deviation to sample standard deviation., *Ann. Math. Stat.* 6 (1935) 214–219.
577 doi:10.1214/aoms/1177732567.
- 578 [47] F.G. Tetreault, A statistical outlier methodology for observed points and lines, Iowa State
579 University, 1965.
- 580 [48] K. Bu, J. V. Cizdziel, L. Reidy, Analysis of herbal supplements for selected dietary minerals and
581 trace elements by laser ablation- and solution-based ICPMS, *Microchem. J.* 106 (2013) 244–
582 249. doi:10.1016/j.microc.2012.07.011.
- 583 [49] H.A.O. Wang, D. Grolimund, L.R. Van Loon, K. Barmettler, C.N. Borca, B. Aeschlimann, D.
584 Günther, Quantitative Chemical Imaging of Element Diffusion into Heterogeneous Media
585 Using Laser Ablation Inductively Coupled Plasma Mass Spectrometry, Synchrotron Micro-X-ray
586 Fluorescence, and Extended X-ray Absorption Fine Structure Spectroscopy, *Anal. Chem.* 83
587 (2011) 6259–6266. doi:10.1021/ac200899x.
- 588 [50] J. Kaiser, M. Galiová, K. Novotný, R. Červenka, L. Reale, J. Novotný, M. Liška, O. Samek, V.
589 Kanický, A. Hrdlička, K. Stejskal, V. Adam, R. Kizek, Mapping of lead, magnesium and copper
590 accumulation in plant tissues by laser-induced breakdown spectroscopy and laser-ablation
591 inductively coupled plasma mass spectrometry, *Spectrochim. Acta - Part B At. Spectrosc.* 64
592 (2009) 67–73. doi:10.1016/j.sab.2008.10.040.
- 593 [51] G.M. Locosselli, K. Chacón-Madrid, M.A. Zezzi Arruda, E. Pereira de Camargo, T.C. Lopes
594 Moreira, C.D. Saldiva de André, P. Afonso de André, J.M. Singer, P.H. Nascimento Saldiva, M.S.
595 Buckeridge, Tree rings reveal the reduction of Cd, Cu, Ni and Pb pollution in the central region
596 of São Paulo, Brazil, *Environ. Pollut.* 242 (2018) 320–328. doi:10.1016/J.ENVPOL.2018.06.098.
- 597 [52] U. Narewski, G. Werner, H. Schulz, C. Vogt, Application of laser ablation inductively coupled
598 mass spectrometry (LA-ICP-MS) for the determination of major, minor, and trace elements in

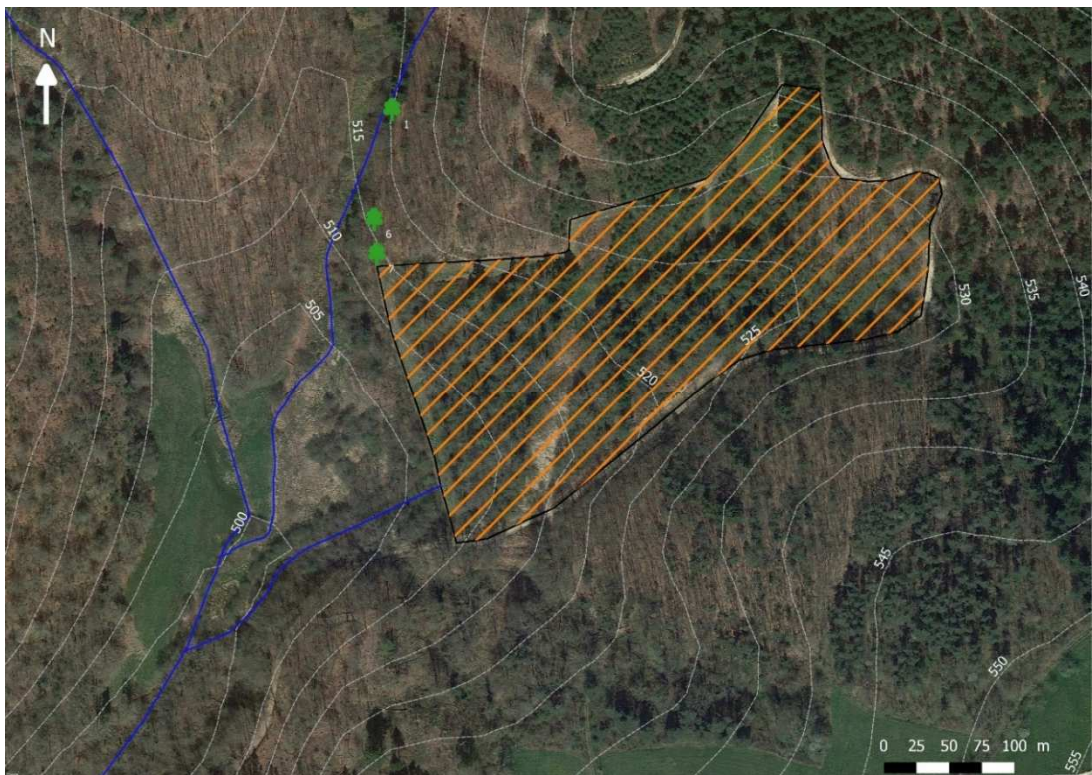
- 599 bark samples, Fresenius. *J. Anal. Chem.* 366 (2000) 167–170. doi:10.1007/s002160050032.
- 600 [53] B. Müller, M. Guillong, Laser Ablation ICP-MS Analysis of Marine Sediments from the
601 Oxfordian (Late Jurassic): A Comparison of Three Preparation Techniques, *Open Mineral. J.* 4
602 (2010) 9–19. <http://benthamscience.com/open/tomj/articles/V004/9TOMJ.pdf>.
- 603 [54] I. Gough, L. and Ridley, Laser Ablation ICP-Mass Spectrometry -- A New Tool for Analyzing
604 Metals in Tree Rings, Version 1., 2004. doi:10.3133/fs20043031.
- 605 [55] T. Prohaska, C. Stadlbauer, R. Wimmer, G. Stingeder, C. Latkoczy, E. Hoffmann, H.
606 Stephanowitz, Investigation of element variability in tree rings of young Norway spruce by
607 laser-ablation-ICPMS, *Sci. Total Environ.* 219 (1998) 29–39. doi:10.1016/S0048-
608 9697(98)00224-1.
- 609



610

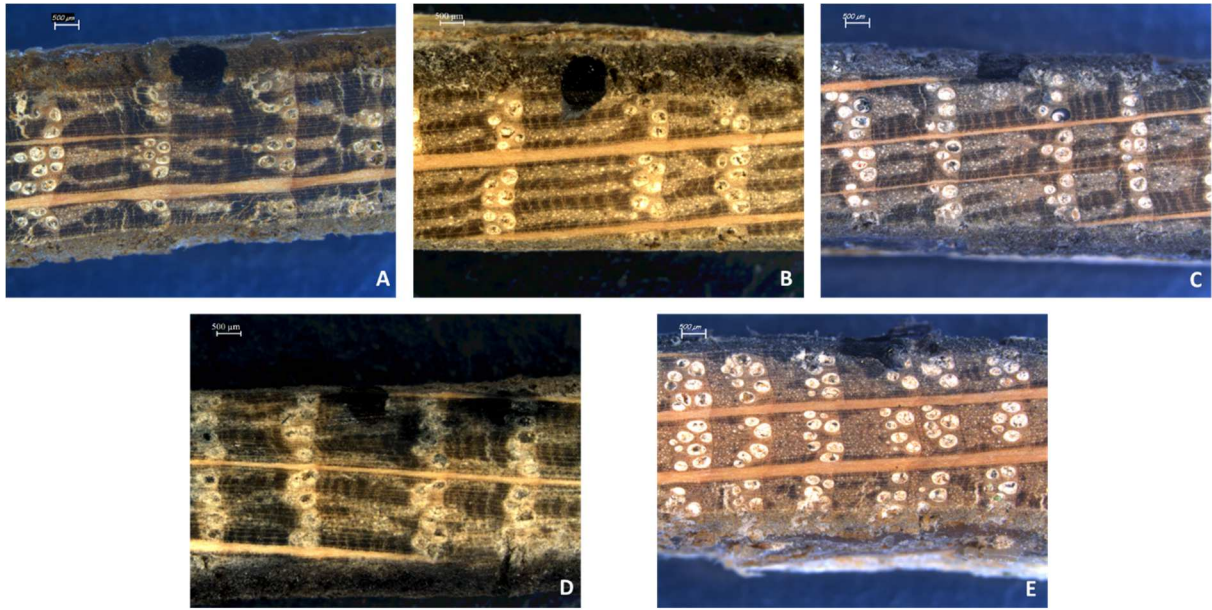
611 **Figure 1:** Location of the radioactive storage site at Rophin (France)

612



613

614 **Figure 2:** Location of the sampled trees (green spots, n=3) around the former Rophin mine (Puy de
 615 Dôme, France). The hatched area indicates mine waste storage.

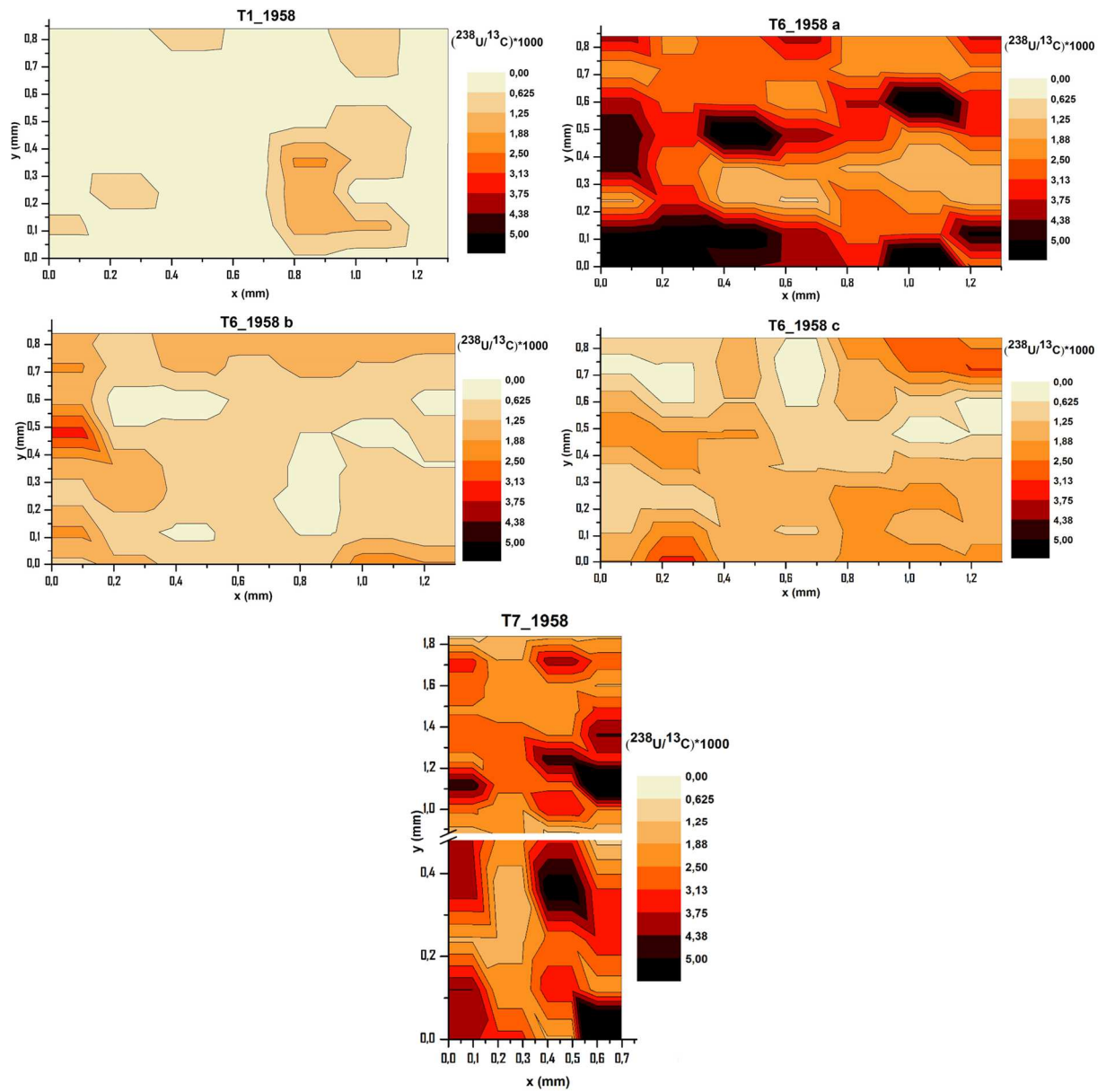


616

617 **Figure 3:** Tree ring samples characterized by a Leica DCF290 HD Digital camera (before ablation): (A)
618 T1; (B) T6-a; (C) T6-b; (D) T6-c; (E) T7

619

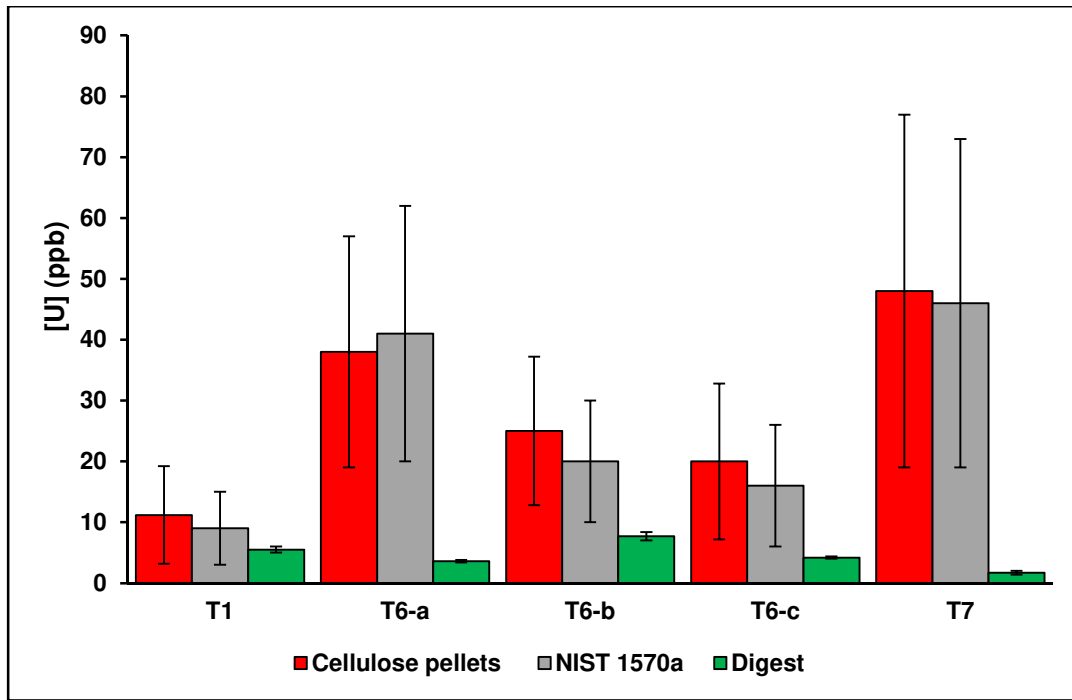
620



621

622 **Figure 4:** 2D mappings of uranium distribution at the tree ring surface

623



624

625 **Figure 5:** Comparison of uranium contents in the tree ring samples using both techniques in LA-HR-
 626 ICP-MS (red and gray) and HR-ICP-MS solution (green)

627 **Table 1:** Operating conditions for the (LA)-HR-ICP-MS technique

Laser ablation device	NWR UP 213
Wavelength	213 nm
Pulse energy	0.5 mJ (50%)
Fluence	10.8 J cm ⁻²
Repetition rate	10 Hz
Spot size diameter	80 μm
Scanning speed	(Pre)-ablation : (30 μm s ⁻¹); 5 μm s ⁻¹
Ablation mode	Line (100 μm)
Number of lines	56
Interline spacing	X = 200 μm ; Y = 120 μm
Washout time	50 s
Warmup time	10 s
Carrier gas flow rate (He)	0.87 L min ⁻¹
Make-up gas flow rate (Ar)	0.92 L min ⁻¹
HR ICP-MS	Thermo Scientific Element XR
RF power	1,200 W
Auxiliary gas flow rate (Ar)	0.84 L min ⁻¹ (LA mode); 0.8 L min ⁻¹ (solution mode)
Cool gas flow rate (Ar)	16 L min ⁻¹
Internal standards	¹³ C (LA mode); ²⁰⁵ Tl (solution mode)
Sampler and skimmer cones	Ni
Acquisition time	60 s (LA mode); 75 s (solution mode)
Detector Mode	Triple
Mass resolution mode	300
Mass window	50%
Runs × passes	55 × 1 (LA mode); 5 × 5 (solution mode)

628

629 **Table 2:** Uranium concentrations in both external standards determined by HR-ICP-MS solution

Sample	[U] (μg kg⁻¹) (± 2σ)	[U] (μg kg⁻¹) (± 2σ)
	Targeted values (gravimetric)	Measured values (HR-ICP-MS)
Point 1	48 ± 2	44 ± 3
Point 2	98 ± 3	102 ± 5
Point 3	203 ± 4	209 ± 13
Point 4	403 ± 7	413 ± 32
<i>NIST 1570a</i>	155* ± 23	166 ± 11

630 *Certified value

631 **Table 3:** Limits of detection (LODs) of uranium by with both methods (LA-ICP-MS and ICP-MS
632 solution)

Samples	LODs	
	LA-HR-ICP-MS (ng kg ⁻¹)	HR-ICP-MS Solution (ng kg ⁻¹)
T1	10	0.3
T6-a	24	0.3
T6-b	23	0.2
T6-c	7	0.2
T7	10	0.5

633

